Original Article

JCBFM

Journal of Cerebral Blood Flow & Metabolism
2021, Vol. 41(12) 3350–3364

DOI: 10.1177/0271678X211036606
journals.sagepub.com/home/jcbfm
SAGE

Common and unique structural plasticity after left and right hemisphere stroke

Yijun Chen[1], Yaya Jiang[1], Xiangyu Kong[1], Chenxi Zhao[1], Suyu Zhong[1], Liyuan Yang[1], Tao Feng[1,2], Shaoling Peng[1], Yanchao Bi[1,3], Maurizio Corbetta[4,5,6,7] and Gaolang Gong[1,3]

Abstract

Strokes to the left and right hemisphere lead to distinctive behavioral profiles. Are left and right hemisphere strokes (LHS and RHS) associated with distinct or common poststroke neuroplasticity patterns? Understanding this issue would reveal hemispheric neuroplasticity mechanisms in response to brain damage. To this end, we investigated poststroke structural changes (2 weeks to 3 months post-onset) using longitudinal MRI data from 69 LHS and 55 RHS patients and 31 demographic-matched healthy control participants. Both LHS and RHS groups showed statistically common plasticity independent of the lesioned hemisphere, including 1) gray matter (GM) expansion in the ipsilesional and contralesional precuneus, and contralesional superior frontal gyrus; 2) GM shrinkage in the ipsilesional medial orbital frontal gyrus and middle cingulate cortex. On the other hand, only RHS patients had significant GM expansion in the ipsilesional medial superior and orbital frontal cortex. Importantly, these common and unique GM changes post-stroke largely overlapped with highly-connected cortical hub regions in healthy individuals. Moreover, they correlated with behavioral recovery, indicating that post-stroke GM volumetric changes in cortical hubs reflect compensatory rather than maladaptive mechanisms. These results highlight the importance of structural neuroplasticity in hub regions of the cortex, along with the hemispheric specificity, for stroke recovery.

Keywords

Left hemisphere stroke, right hemisphere stroke, poststroke plasticity, gray matter volume, voxel-based morphometry

Received 31 March 2021; Revised 18 June 2021; Accepted 7 July 2021

Introduction

Neuroimaging has demonstrated structural and functional changes of brain organization post-stroke related to recovery.[1–4] Damage to left hemisphere (LH) and right hemisphere (RH) produces different functional deficits, e.g., language deficits for LH stroke (LHS)[5] and hemispatial neglects for RH stroke (RHS),[6,7] which may drive specific post-stroke reorganization to support different functional recovery between LHS and RHS patients. When the two hemispheres act as the ipsilesional (or contralesional) hemisphere to unilateral strokes (i.e., LHS or RHS), they may also respond to such ipsilateral (or contralateral) attack differently in nature, due to the anatomical and functional difference between them. In this study, we ask whether LHS and RHS cause different or similar neuroplastic structural changes within the ipsilesional or contralesional hemispheres. Determining whether and how

[1]State Key Laboratory of Cognitive Neuroscience and Learning & IDG/McGovern Institute for Brain Research, Beijing Normal University, Beijing, China
[2]Department of Rehabilitation, The Affiliated Hospital of Xuzhou Medical University, Xuzhou, China
[3]Beijing Key Laboratory of Brain Imaging and Connectomics, Beijing Normal University, Beijing, China
[4]Department of Neuroscience, Neurology Clinic, University of Padua, Padua, Italy
[5]Padova Neuroscience Center, University of Padua, Padua, Italy
[6]Venetian Institute of Molecular Medicine, Padova, Italy
[7]Department of Neurology, Radiology, and Neuroscience, Washington University in St. Louis, St. Louis, USA

Corresponding author:
Gaolang Gong, State Key Laboratory of Cognitive Neuroscience and Learning & IDG/McGovern Institute for Brain Research, Beijing Normal University, #19 Xinjiekouwai Street, Beijing 100875, China.
Email: gaolang.gong@bnu.edu.cn

post-stroke plasticity patterns in the course of recovery differ or overlap for lesions in the two hemispheres will improve our understanding of mechanisms in response to unilateral brain damage, and may guide LHS/RHS dependent or independent stimulation targets.

Functional recovery post-stroke may depend on perilesional plasticity, a shift of activity toward the homologous cortex in the opposite hemisphere, or a change in the balance of excitation-inhibition between hemispheres.[8] Accordingly, neuroimaging studies have reported modulations of activity in these regions post-stroke.[9,10] More controversial is the role of other cortical or subcortical regions that are not strictly related to the lesion site. For instance, patient groups with heterogeneous lesions but similar behavioral deficits manifest robust patterns of activity or connectivity as compared to healthy controls.[11–15] A meta-analysis of chronic aphasia patients with variable lesion location found consistent activation in structurally intact left hemisphere language areas as well as the right hemisphere homotopic regions of the left language network.[16] Together, these findings imply that some neuroplastic changes are independent of an individual's specific lesion site within a given hemisphere. Functional imaging studies strongly support this hypothesis, but it is less clear whether corresponding changes in structure, e.g., regional cortical volume, occur in stroke and whether they relate to recovery of function, and whether they are similar or different in LHS and RHS.

The present study examined longitudinal post-stroke MRI data from two large groups of LHS and RHS patients, who are representative of the clinical stroke population at large and are not preselected based on behavioral deficits or lesion location. We aimed to ascertain: 1) shared longitudinal structural changes of heterogeneous LHS and RHS patients; and 2) common and unique within-group shared longitudinal changes between the two patient groups and their behavioral correlates. We analyzed the longitudinal changes of GMV from 2 weeks to 3 months poststroke, a period of enhanced poststroke structural neuroplasticity.[1,17]

Methods

In the present study, we used a longitudinal stroke dataset, which includes 132 patients with a first symptomatic stroke (19–83 years) and 31 matched healthy controls.[13] The research protocol for original data collection was approved by the Washington University School of Medicine (WUSM) Internal Review Board. Written informed consent was obtained from all participants in accordance with the Helsinki Declaration and procedures established by the Washington University in Saint Louis Institutional Review Board.

Participants

The patient samples are representative of the clinical stroke population at large and were not preselected based on behavioral profile or lesion location. Inclusion criteria were: 1) Age 18 or older; 2) First symptomatic stroke, ischemic or hemorrhagic; 3) Up to two lacunae, clinically silent, less than 15 mm in size on CT scan; 4) Clinical evidence of motor, language, attention, visual, or memory deficits based on neurological examination; 5) Time of enrollment: $<$2 weeks after stroke onset; 6) Awake, alert, and capable of participating in research. Exclusion criteria were detailed in the Supplementary Methods.

For stroke patients, MRI scans were conducted at three time points: 2 weeks, 3 months, and 12 months post onset. Healthy controls were scanned twice, with an interval of approximately 3 months. All MRI scans were performed using a Siemens 3 T Tim-Trio scanner with a standard 12-channel head coil. The MRI parameters are detailed in the Supplementary Methods.

Due to our focus on unilateral lesions, we excluded 4 patients from the dataset who had bilateral lesions. Poor quality of T1-weighted images led to further exclusion of data from 8 patients (5 first visit, 4 second visit, 3 third visit) and 3 healthy controls (1 first scan, 2 second scan). Accordingly, 124 patients, who had at least one successful T1-weighted images across the three visits, were entered into our analyses: the first visit included 68 LHS and 55 RHS patients; the second visit included 54 LHS and 40 RHS patients; the third visit included 46 LHS and 35 RHS patients. For healthy controls, 31 participants were included, 30 for the first visit and 29 for the second visit. Detailed demographic information is listed in Table 1. Given the lack of a third MRI scan for the healthy controls, we focused on the longitudinal analyses of patients' MRI data between the first and second visits.

Neuropsychological tests

Following each scanning session, all participants underwent a battery of neuropsychological tests from four behavioral domains: language, visual attention, memory, and motor. Language was assessed with subtests of the Boston Diagnostic Aphasia Examination (BDAE-III). Visuospatial attention processes were measured with the Posner orienting task, the Star Cancellation subtest of the Behavioral Inattention Test (BIT), and the Mesulam Unstructured Symbol Cancellation Test. Visual and verbal memory were tested with the Brief Visuospatial Memory Test-Revised (BVMT-R) and the Hopkins Verbal Learning Test-Revised (HVLT-R), respectively. The motor battery included a series of tests measuring the

Table 1. Demographic data of participants in the present study.

	LHS patients			RHS patients			Healthy controls	
	2 weeks	3 months	12 months	2 weeks	3 months	12 months	Visit 1	Visit 2
Number of participants	68	54	46	55	40	35	30	29
Age in years	54.0 ± 11.7	54.5 ± 11.1	54.9 ± 10.7	52.2 ± 9.1	53.3 ± 8.6	53.5 ± 7.6	55.0 ± 11.9	54.8 ± 12.0
Gender (M/F)	38/30	30/24	28/18	29/26	22/18	19/16	14/16	15/14
Education in years	13.4 ± 2.7	13.3 ± 2.6	13.8 ± 2.8	13.1 ± 2.3	13.0 ± 2.2	13.1 ± 2.2	13.6 ± 2.6	13.4 ± 2.3
Handedness (R/L)	65/3	52/2	45/1	47/8	33/7	29/6	28/2	27/2
Days post stroke	12.8 ± 3.9	113.8 ± 20.9	395.3 ± 66.1	14.0 ± 5.5	110.6 ± 15.6	384.9 ± 22.1	–	–
Lesion size (cm^3)	25.3 ± 32.3	27.8 ± 44.9	22.5 ± 28.7	38.3 ± 47.8	36.2 ± 42.8	33.6 ± 43.2	–	–

The interval between the two visits of healthy controls was 97 ± 18 days.

upper and lower body functions. For more details, please see Corbetta et al., 2015.[13] For each behavioral domain, a principal component analysis (PCA) with oblique rotation was applied to all within-domain testing scores. This resulted in one main factor for the language, 3 main factors for the attention, 2 main factors for the motor, and 2 main factors for the memory.[13] As in previous work,[18] we only used the first factor of the attention. Therefore, 6 PCA-based scores (covering the four domains) were entered into our behavior-related analyses, representing language, spatial attention, left motor, right motor, verbal memory, and spatial memory.

Lesion site

For each patient, the stroke lesion was manually outlined and the results were validated by two board-certified neurologists who were blind to patient identity and behavioral scores.[13] Based on categorical lesion location, patients were classified into 6 subgroups[13]: cortical (24 LHS, 13 RHS), cortico-subcortical (16 LHS, 16 RHS), subcortical (12 LHS, 16 RHS), white matter only (6 LHS, 1 RHS), brainstem (5 LHS, 6 RHS), cerebellum (5 LHS, 2 RHS). For both patient groups, the distribution of lesion topography is illustrated in Figure 1(a).

Voxel-based morphometry (VBM) processing

We carried out longitudinal VBM analyses using SPM12 (http://www.fil.ion.ucl.ac.uk/spm). To ensure unbiased comparisons between left and right hemispheres, a customized sample-specific symmetric template in MNI space was constructed using the control group.[19] The longitudinal VBM processing included the following procedures: 1) for each participant, an average image across the longitudinal images was generated using the Serial Longitudinal Registration toolbox[20]; 2) the participant-specific average images were bias-corrected and segmented into GM, WM, and cerebrospinal fluid (CSF) probability maps. These tissue-segmented images were then registered to the customized sample-specific symmetric template in the MNI space, resulting in a participant-specific GM probability map in MNI space; 3) the GM probability maps were then modulated with two-fold Jacobian determinants: from the native space of each time point to the participant-average space and from the participant-average space to MNI space. For each participant, this resulted in a GM volume (GMV) map in MNI space for each time point, in which each voxel's value represents its corresponding GMV in the native space. 4) Finally, all of these GMV images were smoothed with an 8-mm full width half maximum

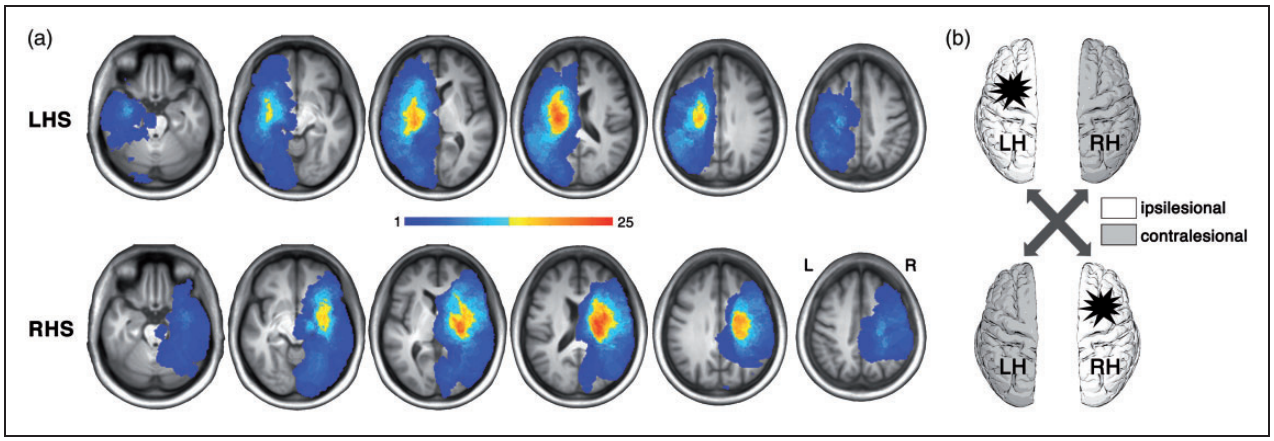

Figure 1. Lesion distribution for LHS and RHS patients. (a) The lesion topography for LHS and RHS patient groups. This map was based on 69 LHS and 55 RHS patients, who had at least one successful MRI acquisition across the three visits. As shown, non-overlapping lesions across subjects exist. (b) The schematic comparison. The statistical maps of longitudinal GMV changes for LHS and RHS groups were compared in terms of the ipsilesional or contralesional hemisphere, respectively. LHS, left hemisphere stroke; RHS, right hemisphere stroke.

Gaussian kernel. In all procedures, each participant's stroke lesion had been masked out.[21] All resultant images of each step were checked by visual inspection.

Identifying longitudinal changes of each patient group

We used a linear mixed-effects model (LMEM) to handle the hierarchical nature of the longitudinal data.[22] Kolmogorov–Smirnov test (K–S test) was used to test the normality of data. Here, the LMEM was applied to evaluate the longitudinal changes of both behavioral scores and voxel-wise GMV from 2 weeks to 3 months post onset. Specifically, the 'fitlme' function in Matlab was used. In the model, "poststroke time" (i.e., the days post onset) and other covariates were modelled as fixed effect and "individual identity" as a random effect. The intercept and slope were allowed to vary across individuals. Specific LMEMs are formulated as below:

$$\begin{aligned} Y_{ij} = {} & \text{intercept} + \beta_1(\text{poststroke time}) \\ & + \beta \ldots (\text{covariates}) + d_{ij} + e_{ij} \end{aligned}$$

Where the intercept and β terms are fixed effects, the d_{ij} is a random effect modeling within-subject dependence, and e_{ij} represents the residual error.

For each patient group, the voxel-wise LMEM analysis was performed within the GM masks of the ipsilesional and contralesional hemispheres, separately. We first generated two symmetric hemispheric GM masks using the control group, and directly applied the hemispheric GM mask to the contralesional hemisphere. For the ipsilesional hemisphere, we excluded the lesioned GM voxels in any LHS or RHS patient from the hemispheric GM mask, because the GMV is unmeasurable for the lesioned voxels. The GM mask for the ipsilesional hemisphere therefore occupies a portion of the entire hemispheric GM mask (~20%), including only the GM voxels that were intact across all stroke patients (see Supplementary Methods for details).

For all measures, the longitudinal poststroke changes were evaluated using the β_1 term. To determine the longitudinal improvement of behavioral performance, we applied the above model, in which age, gender, education, handedness, lesion size, and categorical lesion location were included as covariates. For voxel-wise GMV measures, the LMEMs included age, gender, education, handedness, lesion size, categorical lesion location, and total intracranial volume (ICV) at the first time point as covariates. Controlling for the lesion size and categorical lesion location ensures that the identified GMV changes were not driven by particular lesion and therefore represent shared neuroplastic change across LHS or RHS patients. During the voxel-wise GMV analysis, multiple comparisons were corrected using the random field theory (RFT) method (uncorrected $p < .001$), and clusters with a corrected $p < .05/4$ (2 patient groups $\times$ 2 hemispheres) were considered significant.

Determining common and unique GMV changes to the LHS and RHS groups

After left-right flipping of the LHS group's statistical maps, we statistically evaluated the commonality and uniqueness of the observed clusters between LHS and

RHS groups, in terms of ipsilesional and contralesional hemisphere (Figure 1(b)). To determine the GMV change common to both groups, conjunction analyses were applied to the LHS and RHS statistical maps now classified in terms of ipsilesional and contralesional hemispheres. The FSL-based function of "easythresh_conj.sh" (uncorrected $p < .001$, corrected $p < .05$) was used to estimate the significance of the intersection of two significant clusters (ipsilesional or contralesional) separately from the LHS and RHS group.[23] A significant overlapping ipsilesional or contralesional region in the hemisphere indicates that the longitudinal GMV changes in this region are common to both LHS and RHS groups, ipsilaterally or contralaterally.

If an ipsilateral or contralateral cluster from one patient group (LHS or RHS) did not intersect with any cluster in the other patient group, we tested whether there were significant differences in the beta coefficients of the "poststroke time" between this cluster and its ipsilaterally- or contralaterally-corresponding mask in the other patient group. A permutation test was applied to estimate the significance for such a difference by shuffling the patient group identities. Such a significant difference indicates that the cluster is ipsilaterally or contralaterally unique to its patient group (LHS or RHS).

It should be noted that the identified within-group clusters separately from the LHS or RHS group would not be necessarily classified as common or unique regions here, since they may survive neither statistical significance of determining common and unique changes between the two groups above.

To ascertain whether those observed GMV changes in common and unique regions were specific to stroke patients, we modified the above LMEM by adding a "group" term and a "group × poststroke time" interaction term. In this model, significant interaction indicated different longitudinal GMV change between the patients and healthy controls, therefore supporting the specificity of the observed GMV changes of patients.

Relationship between longitudinal GMV change and behavioral recovery

For all identified common and unique regions above, we evaluated whether the GMV changes (3 months minus 2 weeks poststroke) were significantly correlated with the changes of the impaired behavioral scores in each patient group. Age, gender, education, handedness, lesion size, categorical lesion location, and ICV were included as covariates. The false discovery ratio (FDR) method was applied to correct for multiple comparison, and corrected $p < .05$ was set as the significance level.

For common or unique regions showing a significant correlation with a particular behavioral score, we verified whether the region was associated with this behavior in the existing neuroimaging literature with an ROI-based functional decoding analysis via the Neurosynth decode tools (https://github.com/neurosynth/neurosynth).[24] If yes, this would suggest that the region is involved in this particular behavioral function under both normal and poststroke conditions; if no, it would imply that the region does not typically take part in this behavioral function under normal conditions but becomes involved during poststroke neuroplastic reorganization.

Overlap with cortical hub regions of healthy individuals

In healthy individuals, there exist a minority of hub regions that are highly interconnected with other regions in the brain.[25,26] Hub regions mediate many long-distance connections and are suited to support shared neuroplasticity induced by heterogeneous stroke damage across the brain. We therefore evaluated whether the common and unique regions we identified were located in cortical hub regions. We applied the atlas of intrinsic connectivity of homotopic areas (AICHA) to parcellate the entire cerebral cortex.[27] We then used the WM tractography based on high-quality diffusion MRI data from the Human Connectome Project (HCP) (~1000 healthy participants)[28] to estimate cortical structural connectivity networks (binary/unweighted) of healthy participants.[29] For each AICHA region, the number of connections to all the other AICHA regions within each individual cortical network was calculated and then averaged across all HCP individuals. As did previously,[25] the regions were determined as hubs if their subject-mean number of connections are at least one SD greater than the average across all regions.

Data availability

The MRI and behavioral data are available in the Central Neuroimaging Data Archives at https://cnda.wustl.edu/, reference number: CCIR_00299.

Results

Lesion topography

Figure 1 illustrates the overlapping maps of spatially-normalized lesions in MNI space for the LHS and RHS groups. Given the heterogeneous nature of the included

patients, stroke lesions of both groups were widely distributed across the entire hemisphere. The overall patterns of the two overlapping maps are quite symmetric and significantly spatially correlated ($r = .86$, $p < .0001$), suggesting a matched lesion topography between the LHS and RHS groups. Accordingly, the two groups did not show a significant difference in lesion size (two sample t-test, $t(121) = 1.79$, $p = .08$) or categorical lesion location ($\chi^2(df = 6) = 7.53$, $p = .27$).

Behavioral deficits and longitudinal recovery in both patient groups

The six PCA-based behavioral scores were first compared between each patient group and the HC group using general linear model. The LHS patients' performance at 2 weeks poststroke was significantly worse in language ($t(91) = -3.89$, $p = .0002$), left motor ($t(83) = -3.85$, $p = .0002$), right motor ($t(83) = -4.97$, $p = .000004$), verbal memory ($t(72) = -4.61$, $p = .00002$), and spatial memory ($t(72) = -3.11$, $p = .0026$) but there was only a trend for spatial attention ($t(80) = -1.95$, $p = .06$). The RHS patients' performance was significantly worse in the spatial attention ($t(70) = 2.93$, $p = .0046$), left motor ($t(78) = -5.75$, $p = .0000002$), right motor ($t(78) = -3.67$, $p = .0004$), verbal memory ($t(72) = -2.34$, $p = .022$), and spatial memory ($t(72) = -3.20$, $p = .002$) but not for language ($t(79) = -1.26$, $p = .212$). Only the impaired behavioral scores were entered into subsequent correlation analysis between longitudinal GMV and behavioral changes (LHS group, 5 behavioral scores; RHS group, 5 behavioral scores). For all these impaired behaviors in both groups, the LMEM showed significant improvement at 3 months poststroke (all $ps < .01$).

Longitudinal GMV changes of each patient group

A voxel-wise searchlight was applied to identify local GMV changes between 2 weeks and 3 months post onset. As illustrated in Figure 2, within the GM mask of the ipsilesional hemisphere, we identified 3 LHS clusters (1 of increased GMV, and 2 of decreased GMV) and 4 RHS clusters (2 of increased GMV, and 2 of decreased GMV). The 3 LHS clusters spatially overlapped (in homologous regions) with 1 increased RHS cluster and 2 decreased RHS clusters, respectively. Within the GM mask of the contralesional hemisphere, there were 3 LHS clusters (2 of increased GMV, and 1 of decreased GMV) and 3 RHS clusters (all increased GMV). The two increased LHS clusters showed substantial spatial overlap with the first two largest increased RHS clusters, respectively. These identified significant clusters were detailed in Table 2.

Regardless of the change direction, we calculated the overall volumetric proportion of all identified clusters out of the GM mask for each hemisphere, i.e., the relative size of cortical regions with significant GMV changes in each hemisphere: 4.68% GM regions of the ipsilesional hemisphere and 12.14% GM regions of the contralesional hemisphere for the LHS group; 13.35% GM regions of the ipsilesional hemisphere and 12.56% GM regions of the contralesional hemisphere for the RHS group. The less amount of total GMV changes suggested less overall structural plasticity of the ipsilesional hemisphere of the LHS patients, relative to the other hemispheres.

To verify the shared nature of the observed GMV changes across heterogeneous lesion locations, we tested the significance of the identified clusters in three subgroups of lesion location: cortical, cortico-subcortical, subcortical subgroups. The other three subgroups were not tested due to their small sample size (fewer than 7 RHS/LHS patients). The vast majority of the LHS or RHS clusters showed consistently significant GMV changes from 2 weeks to 3 months post onset in each of the subgroups (Table 2).

Common and unique GMV changes between LHS and RHS groups

The conjunction analysis revealed 5 significant overlapping regions in the contralesional or ipsilesional hemisphere, indicating that the longitudinal GMV changes in these regions are common to both LHS and RHS groups (Figure 3(a) to (e)). Notably, two spatially overlapping clusters that are identified separately from the two groups do not necessarily survive statistical significance of this conjunction analysis.

As illustrated in Figure 3(a) to (c), there were three regions showing increased GMV that were statistically common to both groups: increased contralesional region 1 (Common Contra-Cluster1, Figure 3(a)), consisting of the contralateral precuneus and superior parietal lobule ($p = .001$); increased contralesional region 2 (Common Contra-Cluster2, Figure 3(b)), consisting of the contralateral superior frontal gyrus (SFG, $p = .002$); and increased ipsilesional region 1 (Common Ipsi-Cluster1, Figure 3(c)): the ipsilateral precuneus and superior parietal lobule ($p = .015$). The majority of both LHS and RHS patients showed an increase of raw GMV in these 3 common regions (Common Contra-Cluster1, LHS: 81.1% patients, RHS: 90.0% patients; Common Contra-Cluster2, LHS: 69.8%, RHS: 82.5%; Common Ipsi-Cluster1, LHS: 77.4%, RHS: 80.0%). In addition, two regions consistently showed decreased GMV that was statistically common to both groups: decreased ipsilesional region 2 (Common Ipsi-Cluster2, Figure 3(d)): the

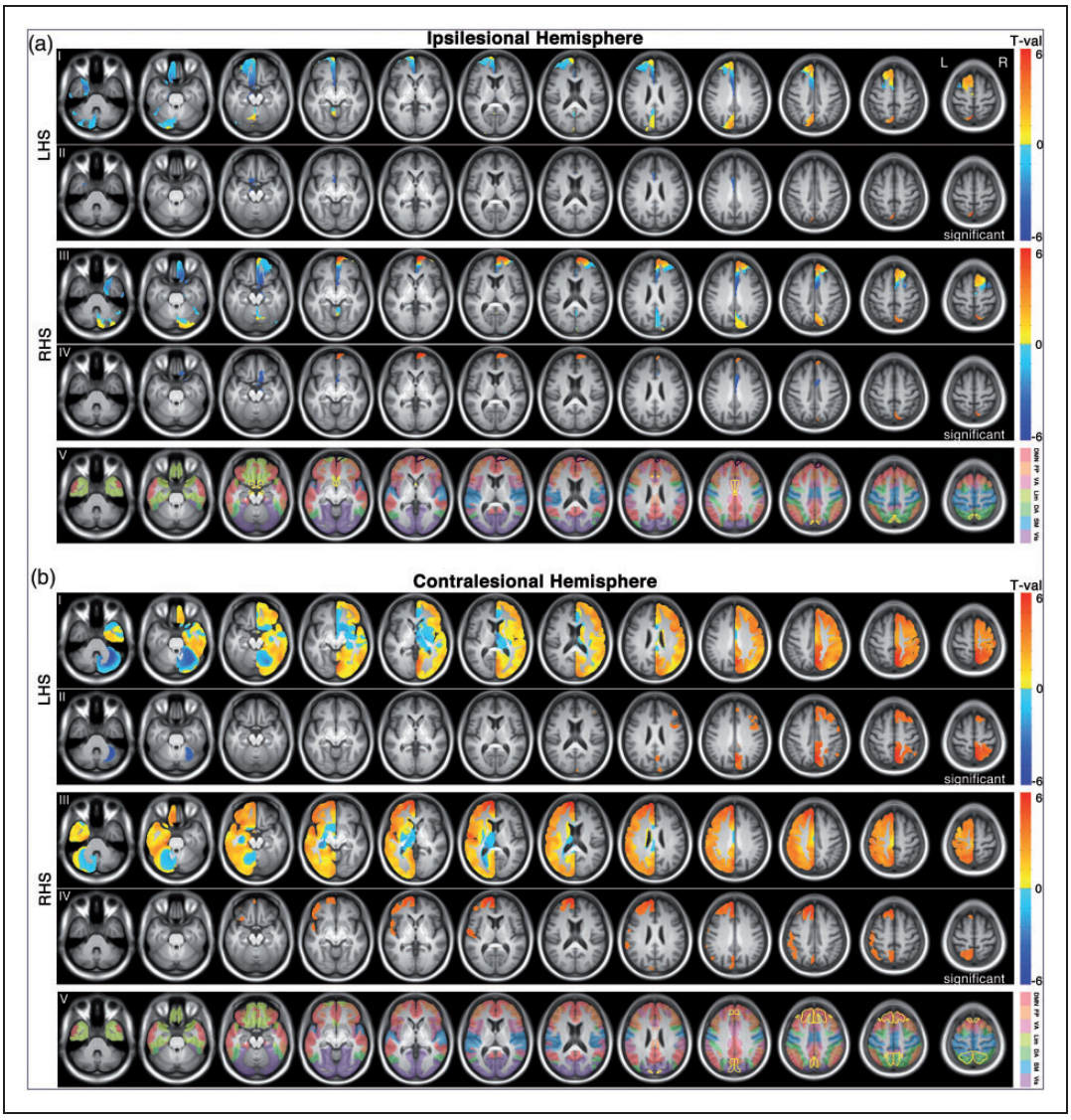

Figure 2. Longitudinal GMV changes (from 2 weeks to 3 months post onset) for both patient groups. (a) The statistical t maps and significant clusters of the ipsilesional hemisphere. For the ipsilesional hemisphere, the searching mask for GMV change includes only the GM voxels that were intact across all patients, therefore just occupying a portion of the entire hemispheric GM mask (~20%). (b) The statistical t maps and significant clusters of the contralesional hemisphere. In both A and B, row I and III represent un-thresholded t maps; Row II and IV represent thresholded t maps (corrected $p < .05$). Notably, the identified within-group clusters separately from the LHS or RHS group may survive neither statistical significance of determining common and unique GMV changes between the two groups, and therefore may not be necessarily classified as common or unique regions in Figures 3 to 5. The contour of common and unique regions between the two groups was displayed in yellow and black, respectively (row V). In the row V, the Yeo's 7 networks were overlapped on the slices.[50] LHS, left hemisphere stroke; RHS, right hemisphere stroke.

posterior portion of the ipsilateral MOFG ($p = .011$) and decreased ipsilesional region 3 (Common Ipsi-Cluster3, Figure 3(e)): the ipsilateral MCC ($p = .013$). As expected, the majority of both LHS and RHS patients showed a decrease of raw GMV in these two regions: Common Ipsi-Cluster2, LHS: 77.4% patients, RHS: 90.0% patients; Common Ipsi-Cluster3, LHS: 71.7%, RHS: 80.0%.

Regarding the uniqueness analysis, a permutation test confirmed that the beta coefficient of the RHS cluster around the ipsilateral medial superior and orbital frontal cortex significantly differed from its corresponding region in the LHS group (10,000 permutations, $p = .003$). Therefore, the observed GMV increase in this ipsilateral RHS cluster was statistically unique to the RHS group, referred to as the unique-RHS ipsilateral region (Unique-RHS Ipsi-Cluster1, Figure 3(f)). The raw GMV of this region showed an increase in the majority of RHS patients but much less in the LHS patients: RHS: 80.0%

Table 2. Clusters showing significant longitudinal GMV changes in the LHS and RHS patient groups, respectively.

	Significant clusters		Size	Corrected p-value	Location (approximate)	p-values in patient sub-groups: Cortical (24 patients)	Cortico-subcortical (16 patients)	Subcortical (12 patients)
LHS	Ipsilesional (LH)	increased cluster 1	1,654 mm^3	0.01	Dorsal precuneus	0.438	**9.2×10^{-5}***	**0.002***
		decreased cluster 1	2,467 mm^3	0.008	Medial orbital frontal gyrus	**0.008***	**8.8×10^{-4}***	**0.011***
		decreased cluster 2	2,153 mm^3	0.01	Middle cingulate cortex	0.089	**8.8×10^{-4}***	**0.011***
	Contralesional (RH)	increased cluster 1	41,691 mm^3	<0.0001	Precuneus & adjacent areas	**0.009***	**0.002***	**0.012***
		increased cluster 2	24,840 mm^3	<0.0001	Large frontal areas	0.129	**4.5×10^{-5}***	**0.006***
		decreased cluster 1	11,684 mm^3	0.001	cerebellum	**0.001***	**0.019***	**0.029***
	Significant clusters		Size	Corrected *p*-value	Location (approximate)	*p*-values in patient sub-groups: Cortical (13 patients)	Cortico-subcortical (16 patients)	Subcortical (16 patients)
RHS	Ipsilesional (RH)	increased cluster 1	7,796 mm^3	0.001	Medial superior/orbital gyri	0.174	**0.005***	**3.0×10^{-5}***
		increased cluster 2	1,742 mm^3	0.01	Precuneus & adjacent areas	**5.8×10^{-4}***	**0.001***	0.158
		decreased cluster 1	4,587 mm^3	0.003	Medial orbital frontal gyrus	**0.025***	**8.4×10^{-4}***	**0.031***
		decreased cluster 2	3,918 mm^3	0.004	Middle cingulate cortex	**0.004***	**5.4×10^{-4}***	**0.040***
	Contralesional (LH)	increased cluster 1	59,356 mm^3	<0.0001	Large frontal areas	**0.020***	**8.7×10^{-6}***	**0.011***
		increased cluster 2	12,879 mm^3	0.001	Precuneus + adjacent areas	**2.1×10^{-5}***	**0.001***	0.972
		increased cluster 3	12,380 mm^3	0.002	Inferior parietal gyrus	**0.020***	**6.4×10^{-4}***	**1.4×10^{-4}***

LH: left hemisphere; RH: right hemisphere; LHS: left hemisphere stroke; RHS: right hemisphere stroke. Three patient subgroups of categorical lesion location were tested: cortical, cortico-subcortical, subcortical subgroups. The other subgroups of categorical lesion location were not tested due to their too small sample size. The vast majority of the clusters identified from all patients also showed significant GMV changes in these subgroups (*$p < .05$). For detailed locations of each cluster, please see Figure 2.
The significance for the values shown in bold is indexed by *.

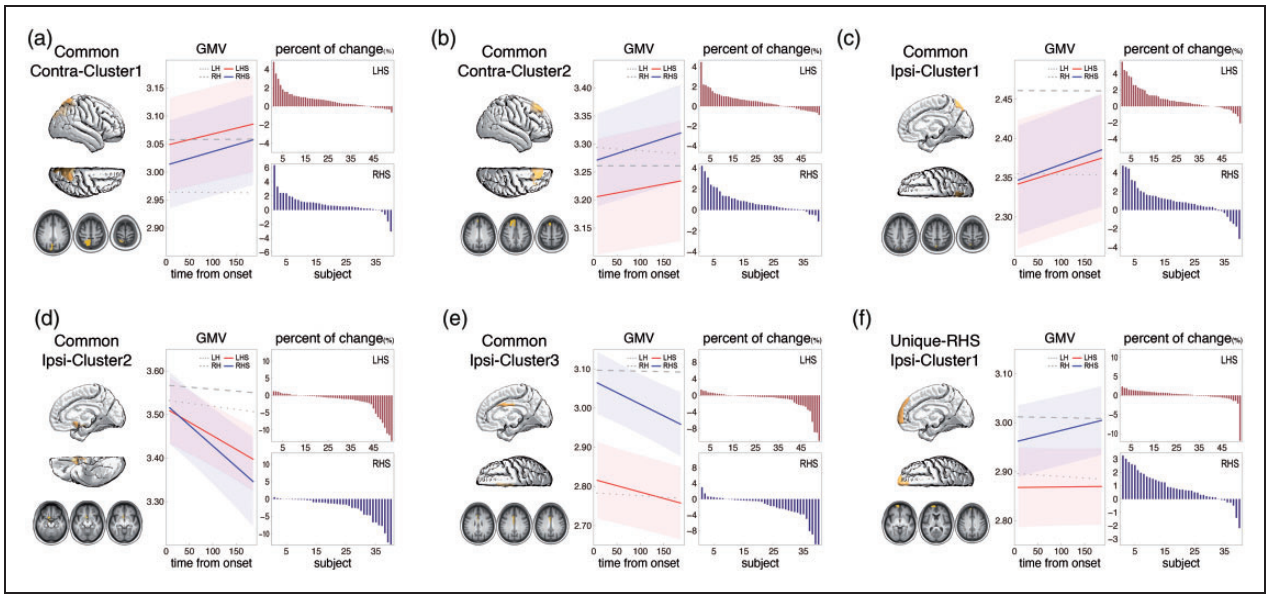

Figure 3. Common and unique GMV changes between LHS and RHS groups. (a) Common GMV increase around the contralesional precuneus (*Common Contra-Cluster1*). (b) Common GMV increase around the contralesional superior frontal gyrus (*Common Contra-Cluster2*). (c) Common GMV increase around the ipsilesional precuneus (*Common Ipsi-Cluster1*). (d) Common GMV decrease around the ipsilesional medial orbital frontal gyrus (*Common Ipsi-Cluster2*). (e) Common GMV decrease around the ipsilesional middle cingulate cortex (*Common Ipsi-Cluster3*). (f) Unique-RHS GMV increase around the ipsilesional anterior medial and superior frontal cortex (*Unique-RHS Ipsi-Cluster1*). Within each panel, the fitted lines for longitudinal GMV changes from the linear mixed-effects model of the patients (in red and blue) and controls (in grey) are illustrated, with the shading representing the 95% confidence interval for the patients. The decreased or increased percent of raw GMV changes of all patients are illustrated as a bar figure in the panel. LH, left hemisphere of controls; RH, right hemisphere of controls; LHS, left hemisphere stroke; RHS, right hemisphere stroke.

patients, LHS: 62.3% patients. There was no other cluster showing statistically unique GMV changes to the LHS or RHS group.

By including the HC group and applying LMEM analysis with a "group × poststroke time" interaction term in the model, we confirmed that all observed common and unique longitudinal GMV changes were specific to stroke patients (the "group × poststroke time" interaction: Common Contra-Cluster1, LHS: $p = .0002$, RHS: $p = .0006$; Common Contra-Cluster2, LHS: $p = .02$, RHS: $p = .00006$; Common Ipsi-Cluster1, LHS: $p = .002$, RHS: $p = .001$; Common Ipsi-Cluster2, LHS: $p = .02$, RHS: $p = .0005$; Common Ipsi-Cluster3, LHS: $p = .047$, RHS: $p = .001$; Unique-RHS Ipsi-Cluster1, RHS: $p = .00009$).

Correlation between longitudinal GMV and behavioral changes

We evaluated 55 correlations between longitudinal GMV and behavioral changes (LHS: 5 common regions against 5 impaired behavioral scores; RHS: 5 common regions and 1 unique region against 5 impaired behavioral scores), and found only 4 significant ones (FDR corrected $p < .05$). Specifically, the GMV increase of the LHS patients in the two common regions of both ipsilateral and contralateral precuneus were positively correlated with the improvement in language scores (i.e., the greater GMV increase the greater language improvement): Common Ipsi-Cluster1 $r = .49$, $p = .002$; Common Contra-Cluster1 $r = .51$, $p = .001$ (Figure 4(a)). In addition, the RHS group showed two significant negative correlations between the GMV decreases in the two ipsilateral common regions and improvement of left motor scores: Common Ipsi-Cluster2 $r = -.75$, $p = .00002$; Common Ipsi-Cluster3 $r = -.73$, $p = .00004$ (Figure 4(b)). Given the negative direction of the GMV change, these negative correlations indicate that more GMV decrease was associated with stronger improvement of the left motor ability in RHS patients.

For the two language-correlated common regions of the LHS patients, we tested their association with the term "language" in the Neurosynth database and did not find a significant association (Common Ipsi-Cluster1: ipsilateral precuneus, $p = .30$; Common Contra-Cluster1: contralateral precuneus, $p > .99$). For the two motor-correlated ipsilateral common regions, we estimated their association with the term "motor" in the Neurosynth database. The association was significant for the ipsilateral common region of the MCC (Common Ipsi-Cluster3, $p < .0001$) but not for

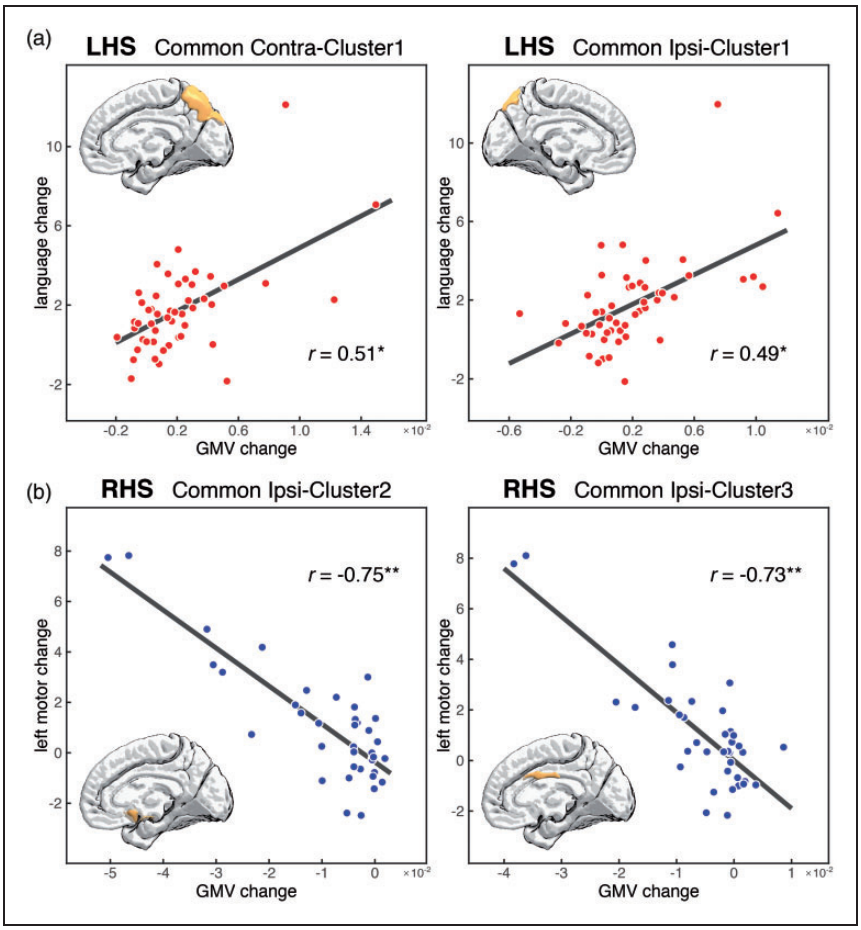

Figure 4. Significant correlations between longitudinal GMV of identified common and unique regions and behavioral changes. (a) Significant positive correlation between GMV increase of the contralesional and ipsilesional precuneus with language improvement in LHS patients. Notably, the correlations remain significant after removing the outlier patient on the top (contralesional precuneus: r =.36, p =.03; ipsilesional precuneus: r =.40, p =.01). (b) Significant negative correlations between GMV decrease of the ipsilesional medial orbital frontal gyrus and middle cingulate cortex with left motor improvement in RHS patients. *p <.01; **p <.0001. LHS, left hemisphere stroke; RHS, right hemisphere stroke.

the ipsilateral common region of the MOFG (Common Ipsi-Cluster2, p > .99) of the RHS patients. These results suggested that bilateral precuneus don't typically take part in language function under normal conditions but become involved during poststroke neuroplastic reorganization in LHS patients, so does the motor function of the ipsilateral MOFG for RHS patients.

Overlap with cortical hub regions of healthy individuals

We used the HCP dataset to identify hub regions of the cortical structural network of healthy participants at the group level. The identified cortical hub regions (including the precuneus and prefrontal cortex) are illustrated in Figure 5. All common and unique regions except for the ipsilateral MOFG, overlapped with at least one cortical hub region. In particular, the two common plastic regions of the bilateral precuneus showed substantial overlap with multiple cortical hub regions. The percentage of hub area for each intersected common or unique region was nontrivial (Common Contra-Cluster1, LHS: 51.3%, RHS: 62.7%; Common Contra-Cluster2, LHS: 42.5%, RHS: 36.4%; Common Ipsi-Cluster1, LHS: 72.3%, RHS: 31.9%; Common Ipsi-Cluster3, LHS: 3.6%, RHS: 23.6%; Unique-RHS Ipsi-Cluster1, RHS: 15.1%).

Validation and control results

To validate our results, we reran the VBM analyses after applying 4 mm and 12 mm smoothing kernels to the GMV maps. All statistical results from these

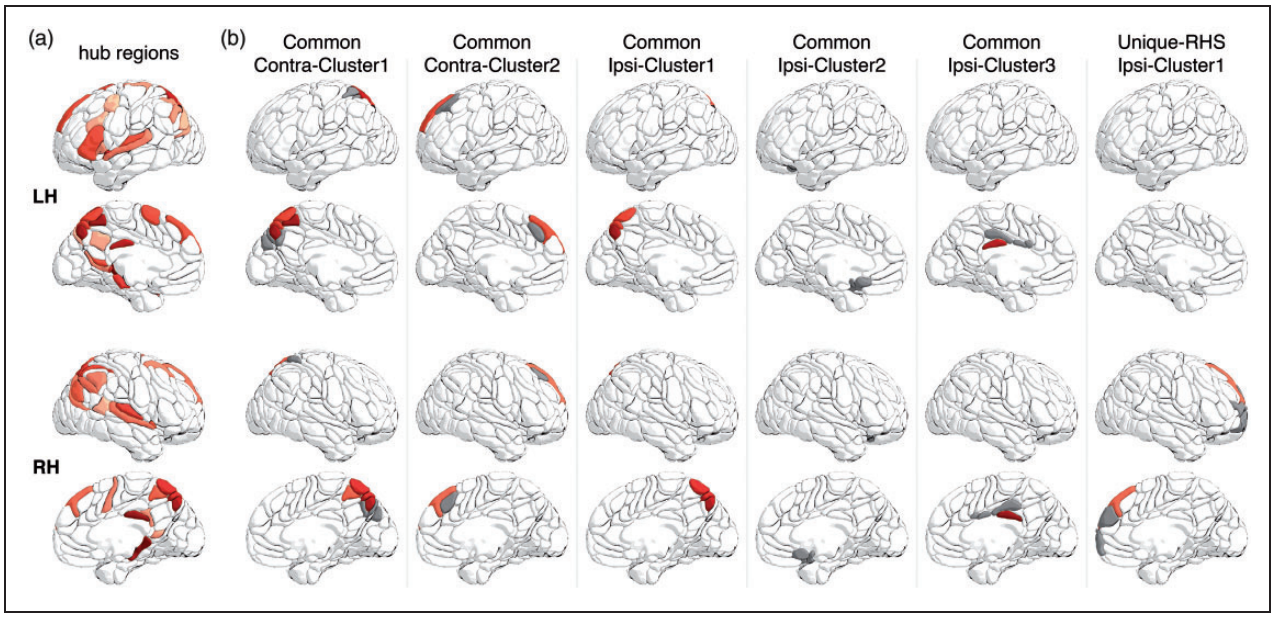

Figure 5. Overlap of the identified common and unique regions with cortical hub regions in healthy individuals. (a) Cortical hub regions. Hub regions are denoted by red color, with darker red representing a stronger hub (i.e., more connections). (b) The intersection of AICHA regions with all identified common and unique region (Figure 3). Hub regions are highlighted in the same red color as in A and non-hub regions are denoted by grey color.

re-analyses are quite similar to our current ones (see Supplementary Figures 2 and 3).

To evaluate the impact of the matched lesion topography between the LHS and RHS groups on the results, we excluded a subset of patients to make a better or worse matched lesion topography between the two groups, and then reran the entire analyses (see Supplementary Methods for details). Based on the subset of patients with either better or worse matched lesion topography, both groups showed quite similar ipsilesional and contralesional t maps with our main results (Supplementary Figures 4 and 5), and the voxel-wise t values are strongly correlated with the current ones based on all patients (the better matching: ipsilesional: LHS, $r = .91$, RHS, $r = .99$; contralesional: LHS, $r = .97$, RHS, $r = .98$; the worse matching: ipsilesional: LHS, $r = .95$; RHS, $r = .98$; contralesional: LHS, $r = .95$; RHS, $r = .95$). These result suggested a limited impact of the matched lesion topography between the two groups on our findings.

For our identified common and unique neuroplastic regions, we additionally assessed their GMV changes from 3 months to 12 months poststroke, using the same LMEM for identifying GMV changes from 2 weeks to 3 months. For both patient groups, the 3 increased common regions (Common Contra-Cluster1, LHS: $p = .48$, RHS: $p = .85$; Common Contra-Cluster2, LHS: $p = .80$, RHS: $p = .51$; Common Ipsi-Cluster1, LHS: $p = .47$, RHS: $p = .65$) and the unique region (Unique-RHS Ipsi-Cluster1, RHS: $p = .07$) didn't show significant changes, suggesting that the GMV increase is a non-transient and stable effect. In contrast, the two decreased common regions (Common Ipsi-Cluster2, LHS: $p = .005$, RHS: $p = .007$; Common Ipsi-Cluster3, LHS: $p = .0002$; RHS: $p < .0001$) showed continuing significant GMV decrease. The specificity of these results to stroke patients could not be evaluated due to the lack of a third time point of data from healthy controls.

Finally, we made a cross-sectional voxel-wise GMV comparison between LHS/RHS and HC groups using general linear models (the first visit: LHS vs. HC, RHS vs. HC; the second visit: LHS vs. HC, RHS vs. HC). The models included age, gender, education, handedness, and ICV as covariates. For all these comparisons we did not find any significant results (see Supplementary Figure 6). This highlights the sensitivity of longitudinal analyses for studying poststroke neuroplastic changes.

Discussion

Using longitudinal post-stroke structural MRI data, we thoroughly investigated common and unique structural brain changes in heterogeneous LHS and RHS patients, by ipsilesional and contralesional hemispheres. We first demonstrated post-stroke specific and within-group shared longitudinal GMV

decrease/increase across patients with heterogeneous lesions. Based on these within-group shared GMV changes, we further revealed a set of GMV changes that were statistically common to both LHS and RHS groups, including: 1) GMV increases of the ipsilateral precuneus and the contralateral precuneus and SFG, and 2) GMV decreases of the ipsilateral MOFG and MCC. In contrast, the GMV increase of the ipsilateral medial superior and orbital frontal cortex was statistically unique to the RHS patients. These identified common and unique regions are largely located around the highly-connected cortical hub regions in healthy individuals. Finally, the GMV increase in the bilateral precuneus was correlated with better language recovery in LHS patients and the GMV decease of the ipsilateral MCC and MOFG was correlated with better motor recovery in RHS patients.

Ipsilaterally and contralaterally shared GMV changes across heterogeneous patients

By contrast to our current study, the majority of previous studies on poststroke structural changes recruited patients with homogeneous lesions or behavioral deficits, adopting cross-sectional comparisons between patient and healthy control groups. Despite these discrepancies, the following compatible results between ours and previous studies were obtained: poststroke increase of GMV or thickness around the ipsilateral, contralateral, or bilateral precuneus,[17,30,31] increase of GMV or thickness around the contralateral prefrontal, orbital frontal and middle frontal cortices, decrease of GMV in the contralateral cerebellum,[17,30,32–35] and decrease of GMV around the ipsilateral cingulate cortex.[17]

Microstructurally, candidate mechanisms for GMV increase in the intact brain tissue include neurogenesis, gliogenesis, synaptogenesis and changes in neuronal morphology, and vascular changes.[36] While the axonal growth, dendritic arborization and spine remodeling are seen in the ipsilesional and contralesional hemisphere,[37,38] glial events and angiogenesis are less common in the contralesional hemisphere.[39] In contrast, the GMV decrease likely represents a secondary neural degeneration following stroke, possibly due to Wallerian degeneration and long-term insufficient blood supply in the ipsilesional hemisphere.[40,41] The secondary degeneration reflected by GMV decrease is not necessarily harmful and may be beneficial for poststroke functional recovery as in the case of the correlation with motor recovery found in our study, suggesting a beneficial nature of structural neuroplastic changes to functional recovery.

Since our observed GMV changes in the LHS or RHS group represent shared GMV changes across heterogeneous patients, these GMV changes should also be expected for a group of LHS or RHS patients with more homogeneous lesion topography. This was verified in our patient subgroups with cortical, cortico-subcortical, or subcortical topography (Table 2). It should be noted that the existence of shared GMV changes across heterogeneous patients is not mutually-exclusive with the classical hypotheses of lesion-site dependent neuroplasticity following a unilateral stroke, e.g., the perilesional hypothesis, laterality-shift hypothesis, and interhemispheric disinhibition hypothesis.[8] Rather, it is likely that the poststroke neuroplasticity of each individual patient involves both individual-specific (e.g., lesion-site dependent) and hemispheric-shared brain changes across patients.

Commonality and uniqueness of ipsilateral and contralateral GMV changes between LHS and RHS patients

The stroke hemisphere has been long considered as a critical determinant for poststroke functional deficits. To our knowledge, the present study provides the first experimental data directly demonstrating the commonality and uniqueness of poststroke longitudinal structural changes between LHS and RHS patients. In a few cross-sectional VBM studies, group results from LHS and RHS patients separately (each relative to healthy controls) have been qualitatively summarized, and very few common results were found between the two groups.[30,42] This discrepancy may relate to their cross-sectional study paradigm and patient selection.

The observed ipsilateral and contralateral GMV changes common to both LHS and RHS groups indicate similar and symmetric neuroplasticity between the two hemispheres in response to unilateral brain damage. Strong evidence has demonstrated that both hemispheres are highly plastic and may work relatively independently. For example, patients after callosotomy or hemispherectomy can manifest well-preserved brain structure and function.[43] On the other hand, we did observe ipsilateral frontal structural plasticity unique to RHS patients. This asymmetric poststroke change suggests more plasticity and structural flexibility of the right frontal cortex relative to its left homotopic area, which may relate to specific structural and functional asymmetries around frontal areas in healthy people.[44,45]

Due to the hemispheric dominance of different behavioral domains, the common ipsilateral or contralateral brain changes do not necessarily lead to similar behavioral consequences between LHS and RHS patients. In line with this idea, our observed behavioral correlations indicate that ipsilateral and contralateral precuneus GMV correlates with language recovery in

LHS patients, but not in RHS patients. This seems to reflect post-stroke functional reorganization as the precuneus is not associated with language based on the Neurosynth database. It is likely that bilateral precuneus changes support behavioral functions other than language in RHS patients. In addition, greater GMV decrease of the ipsilateral MOFG and MCC was associated with better motor recovery in RHS patients but not in LHS patients, further supporting asymmetric neural processes underlying different functional recovery between RHS and LHS patients. This intriguing observation of similar brain changes supporting functional recovery of different behaviors warrants further investigation between LHS and RHS patients.

Notably, the regions we observed with common and unique GMV changes largely overlap with highly-connected cortical hub areas in healthy individuals. Using a pooled meta-analysis across 26 brain disorders (not including brain stroke), Crossley and colleagues recently demonstrated that hub regions are more likely to show anatomical abnormalities than non-hub regions in many brain disorders.[26] This pattern was interpreted as a higher vulnerability of hub regions to a diverse range of pathogenic processes, possibly due to their connections with widely distributed areas across the entire brain. Interestingly, our findings here suggest that a set of cortical hub regions (e.g., bilateral precuneus and SFG) are unlikely to be damaged by unilateral strokes,[46] possibly due to their distance from brain arteries. Moreover, these hub regions play active roles in poststroke neuroplasticity to support functional recovery of particular behaviors (e.g., language). The connections with widely-distributed areas may facilitate the responsiveness of hub regions to heterogeneous stroke attacks across the brain. The functional adaptability and capability of these hub regions make it possible to compensate for various functional deficits from heterogeneous stroke patients.[46]

General implications

First, the common regions we observed may serve as general ipsilateral and contralateral stimulation targets when treating heterogeneous LHS or RHS stroke patients. Given the observed unique-RHS ipsilateral region, the RHS patients also have a unique candidate stimulating target in the right hemisphere. Treatment targeting these patient-shared targets should be complementary to any individualized treatment, jointly boosting functional recovery. Future intervention studies are needed to evaluate the effectiveness of such treatments. Next, our study highlighted the commonality and uniqueness between left and right brain-damaged patients. The analysis framework we established can be applied directly to other brain disorders affecting unilateral brain structures. Finally, our analyses demonstrated the sensitivity of longitudinal analyses and the relative insensitivity of cross-sectional comparisons in studying poststroke neuroplasticity. Longitudinal investigations minimize the confounding effects of inter-individual variability and other mixed pathologies by using patients as their own controls and therefore are essential to reveal the dynamic processes following brain injury.

Limitation and future work

There have been a number of reported poststroke changes in functional activity, functional connectivity, WM connectivity, and brain networks.[47–49] Future studies are needed to reveal how the poststroke changes of different modalities are related and jointly support functional recovery. Next, our findings are limited to the poststroke period from 2 weeks to 3 months. The control analyses further showed unchanged GMV of those observed regions from 3 months to 12 months poststroke, suggesting that the observed structural changes ended before 3 months poststroke. Further studies with more longitudinal MRI data between 1–2 weeks and 3 months are warranted to determine how early the observed structural changes are completed. Finally, our findings are based on adult stroke patients and are unlikely applicable to pediatric stroke patients. The pediatric structural plasticity following a left or right stroke deserves investigation in the future.

Funding

The author(s) disclosed receipt of the following financial support for the research, authorship, and/or publication of this article: This work is supported by the National Natural Science Foundation of China grant (82021004, 91732101, G.G.). M.C. is funded by National Institutes of Health grant (R01 NS095741); FLAGERA JTC 2017; Dipartimento Eccellenza del MIUR Neuro-DiP; and Progetto Strategico UniPD. Some of our data were provided by the Human Connectome Project, WU-Minn Consortium (1U54MH091657).

Declaration of conflicting interests

The author(s) declared no potential conflicts of interest with respect to the research, authorship, and/or publication of this article.

Authors' contributions

G.G. conceived the study. Y.C. performed the main analyses. S.Z., C.Z. and L.Y. performed the structural network analyses. S.P. provided support with the Neurosynth. Y.J. and X. K. provided support for the behavioral data. G.G. and Y.C.

wrote the manuscript. M.C., Y.B. and T.F. revised the manuscript. All authors critically reviewed and approved the manuscript.

ORCID iD

Xiangyu Kong https://orcid.org/0000-0002-8867-6982

Supplemental material

Supplemental material for this article is available online.

References

1. Cramer SC. Repairing the human brain after stroke: I. Mechanisms of spontaneous recovery. *Ann Neurol* 2008; 63: 272–287.
2. Grefkes C and Fink GR. Reorganization of cerebral networks after stroke: new insights from neuroimaging with connectivity approaches. *Brain* 2011; 134: 1264–1276.
3. Baldassarre A, Ramsey LE, Siegel JS, et al. Brain connectivity and neurological disorders after stroke. *Curr Opin Neurol* 2016; 29: 706–713.
4. Sampaio-Baptista C, Sanders Z-B and Johansen-Berg H. Structural plasticity in adulthood with motor learning and stroke rehabilitation. *Annu Rev Neurosci* 2018; 41: 25–40.
5. Broca P. Localisation des fonctions cérébrales: Siége de langage articulé. *Bull Société D'Anthropologie Paris* 1863; 4: 200–208.
6. Critchley M. *The parietal lobes*. London: Edward Arnold; 1953.
7. Corbetta M and Shulman GL. Spatial neglect and attention networks. *Annu Rev Neurosci* 2011; 34: 569–599.
8. Geranmayeh F, Brownsett SL and Wise RJ. Task-induced brain activity in aphasic stroke patients: what is driving recovery? *Brain* 2014; 137: 2632–2648.
9. Thiel A, Schumacher B, Wienhard K, et al. Direct demonstration of transcallosal disinhibition in language networks. *J Cereb Blood Flow Metab* 2006; 26: 1122–1127.
10. Hope TMH, Leff AP, Prejawa S, et al. Right hemisphere structural adaptation and changing language skills years after left hemisphere stroke. *Brain* 2017; 140: 1718–1728.
11. He BJ, Snyder AZ, Vincent JL, et al. Breakdown of functional connectivity in frontoparietal networks underlies behavioral deficits in spatial neglect. *Neuron* 2007; 53: 905–918.
12. Carter AR, Astafiev SV, Lang CE, et al. Resting interhemispheric functional magnetic resonance imaging connectivity predicts performance after stroke. *Ann Neurol* 2010; 67: 365–375.
13. Corbetta M, Ramsey L, Callejas A, et al. Common behavioral clusters and subcortical anatomy in stroke. *Neuron* 2015; 85: 927–941.
14. Siegel JS, Ramsey LE, Snyder AZ, et al. Disruptions of network connectivity predict impairment in multiple behavioral domains after stroke. *Proc Natl Acad Sci U S A* 2016; 113: E4367–E4376.
15. Siegel JS, Seitzman BA, Ramsey LE, et al. Re-emergence of modular brain networks in stroke recovery. *Cortex* 2018; 101: 44–59.
16. Turkeltaub PE, Messing S, Norise C, et al. Are networks for residual language function and recovery consistent across aphasic patients? *Neurology* 2011; 76: 1726–1734.
17. Fan F, Zhu C, Chen H, et al. Dynamic brain structural changes after left hemisphere subcortical stroke. *Hum Brain Mapp* 2013; 34: 1872–1881.
18. Baldassarre A, Ramsey L, Rengachary J, et al. Dissociated functional connectivity profiles for motor and attention deficits in acute right-hemisphere stroke. *Brain* 2016; 139: 2024–2038.
19. Kurth F, Gaser C and Luders E. A 12-step user guide for analyzing voxel-wise gray matter asymmetries in statistical parametric mapping (SPM). *Nat Protoc* 2015; 10: 293–304.
20. Ashburner J and Ridgway GR. Symmetric diffeomorphic modeling of longitudinal structural MRI. *Front Neurosci* 2013; 6: 197.
21. Crinion J, Ashburner J, Leff A, et al. Spatial normalization of lesioned brains: performance evaluation and impact on fMRI analyses. *NeuroImage* 2007; 37: 866–875.
22. Pinheiro J and Bates D. *Mixed-effects models in S and S-PLUS*. Springer Science & Business Media, 2006.
23. Nichols T, Brett M, Andersson J, et al. Valid conjunction inference with the minimum statistic. *Neuroimage* 2005; 25: 653–660.
24. Yarkoni T, Poldrack RA, Nichols TE, et al. Large-scale automated synthesis of human functional neuroimaging data. *Nat Methods* 2011; 8: 665–670.
25. Gong G, He Y, Concha L, et al. Mapping anatomical connectivity patterns of human cerebral cortex using in vivo diffusion tensor imaging tractography. *Cereb Cortex* 2009; 19: 524–536.
26. Crossley NA, Mechelli A, Scott J, et al. The hubs of the human connectome are generally implicated in the anatomy of brain disorders. *Brain* 2014; 137: 2382–2395.
27. Joliot M, Jobard G, Naveau M, et al. AICHA: an atlas of intrinsic connectivity of homotopic areas. *J Neurosci Methods* 2015; 254: 46–59.
28. Van Essen DC, Ugurbil K, Auerbach E, et al. The human connectome project: a data acquisition perspective. *Neuroimage* 2012; 62: 2222–2231.
29. Zhong S, Wei L, Zhao C, et al. Interhemispheric relationship of genetic influence on human brain connectivity. *Cereb Cortex* 2021; 31: 77–88.
30. Jiang L, Liu J, Wang C, et al. Structural alterations in chronic capsular versus pontine stroke. *Radiology* 2017; 285: 214–222.
31. Liu H, Peng X, Dahmani L, et al. Patterns of motor recovery and structural neuroplasticity after basal ganglia infarcts. *Neurology* 2020; 95: e1174–e1187.
32. Kraemer M, Schormann T, Hagemann G, et al. Delayed shrinkage of the brain after ischemic stroke: preliminary observations with Voxel-Guided morphometry. *J Neuroimaging* 2004; 14: 265–272.
33. Dang C, Liu G, Xing S, et al. Longitudinal cortical volume changes correlate with motor recovery in patients

after acute local subcortical infarction. *Stroke* 2013; 44: 2795–2801.
34. Abela E, Seiler A, Missimer JH, et al. Grey matter volumetric changes related to recovery from hand paresis after cortical sensorimotor stroke. *Brain Struct Funct* 2015; 220: 2533–2550.
35. Xing S, Lacey EH, Skipper-Kallal LM, et al. Right hemisphere grey matter structure and language outcomes in chronic left hemisphere stroke. *Brain* 2016; 139: 227–241.
36. Zatorre RJ, Fields RD and Johansen-Berg H. Plasticity in gray and white: neuroimaging changes in brain structure during learning. *Nat Neurosci* 2012; 15: 528–536.
37. Schallert T, Leasure JL and Kolb B. Experience-Associated structural events, subependymal cellular proliferative activity, and functional recovery after injury to the central nervous system. *J Cereb Blood Flow Metab* 2000; 20: 1513–1528.
38. Johansson BB. Functional and cellular effects of environmental enrichment after experimental brain infarcts. *Restor Neurol Neurosci* 2004; 22: 163–174.
39. Ergul A, Alhusban A and Fagan SC. Angiogenesis: a harmonized target for recovery after stroke. *Stroke* 2012; 43: 2270–2274.
40. Fierstra J, Poublanc J, Han JS, et al. Steal physiology is spatially associated with cortical thinning. *J Neurol Neurosurg Psychiatry* 2010; 81: 290–293.
41. Thomalla G, Glauche V, Weiller C, et al. Time course of Wallerian degeneration after ischaemic stroke revealed by diffusion tensor imaging. *J Neurol Neurosurg Psychiatry* 2005; 76: 266–268.
42. Diao Q, Liu J, Wang C, et al. Gray matter volume changes in chronic subcortical stroke: a cross-sectional study. *NeuroImage Clin* 2017; 14: 679–684.
43. Devlin AM. Clinical outcomes of hemispherectomy for epilepsy in childhood and adolescence. *Brain* 2003; 126: 556–566.
44. Toga AW and Thompson PM. Mapping brain asymmetry. *Nat Rev Neurosci* 2003; 4: 37–48.
45. Hervé P-Y, Zago L, Petit L, et al. Revisiting human hemispheric specialization with neuroimaging. *Trends Cogn Sci* 2013; 17: 69–80.
46. Cavanna AE and Trimble MR. The precuneus: a review of its functional anatomy and behavioural correlates. *Brain* 2006; 129: 564–583.
47. Forkel SJ, Thiebaut de Schotten M, Dell'Acqua F, et al. Anatomical predictors of aphasia recovery: a tractography study of bilateral perisylvian language networks. *Brain* 2014; 137: 2027–2039.
48. Lunven M, Thiebaut De Schotten M, Bourlon C, et al. White matter lesional predictors of chronic visual neglect: a longitudinal study. *Brain* 2015; 138: 746–760.
49. Stockert A, Wawrzyniak M, Klingbeil J, et al. Dynamics of language reorganization after left temporo-parietal and frontal stroke. *Brain* 2020; 143: 844–861.
50. Thomas Yeo BT, Krienen FM, Sepulcre J, et al. The organization of the human cerebral cortex estimated by intrinsic functional connectivity. *J Neurophysiol* 2011; 106: 1125–1165.